https://doi.org/10.5194/cp-2020-19
Preprint. Discussion started: 24 February 2020

Climate of the Past Discussions

High-frequency climate oscillations in the Holocene from a coastal-dome ice core in east central Greenland

Abigail G. Hughes[1], Tyler R. Jones[1], Bo M. Vinther[2], Vasileios Gkinis[2], C. Max Stevens[3], Valerie Morris[1], Bruce H. Vaughn[1], Christian Holme[2], Bradley R. Markle[4], and James W. C. White[1]

[1]Institute of Arctic and Alpine Research, University of Colorado Boulder, Boulder, Colorado, USA
[2]Physics of Ice, Climate and Earth, The Niels Bohr Institute, University of Copenhagen, Copenhagen, Denmark
[3]Department of Earth and Space Sciences, University of Washington, Seattle, Washington, USA
[4]California Institute of Technology, Pasadena, California, USA

Correspondence: Abigail G. Hughes (abigail.hughes@colorado.edu)

Abstract. An ice core drilled on the Renland Ice Cap in east-central Greenland contains a continuous climate record dating through the last glacial period. The Renland record is valuable because the coastal environment is more likely to reflect regional sea surface conditions, compared to inland Greenland ice cores that capture synoptic variability. Here we present the δ^{18}O water isotope record for the Holocene, in which decadal-scale climate information is retained for the last 8 ka, and the annual water isotope signal is preserved throughout the last 2.6 ka. To investigate regional climate information preserved in the water isotope record, we apply spectral analysis techniques to a 300-year moving window to determine the mean strength of varying frequency bands through time. The strength of interannual frequency bands decays rapidly, but we find that the mean 15-20 year δ^{18}O variability exhibits a millennial-scale cycle in line with the well-known Bond Cycle. Comparison to other North Atlantic proxy records suggests that the 15-20 year variability may reflect fluctuating sea ice conditions throughout the Holocene, driven by changes in the strength of the Atlantic Meridional Overturning Circulation. Additional analysis of the seasonal signal over the last 2.6 ka reveals that the winter δ^{18}O signal has experienced a decreasing trend, while the summer signal has predominantly remained stable. The winter trend likely corresponds to an increase in Arctic sea ice cover, driven by a decrease in total annual insolation. In the context of anthropogenic climate change, the winter trend may have important implications for feedback processes as sea ice retreats in the Arctic.

1 Introduction

Ice core records are powerful archives of past climate change, containing hundreds of thousands of years of climate information. Greenland ice core records are valuable for determining a more comprehensive picture of regional North Atlantic climate patterns throughout the Holocene and last glacial period. Recent developments in Continuous Flow Analysis and cavity ring-down spectroscopy allow for detection of high frequency signals in ice core water isotopes. These measurement techniques were used in analysis of the Renland ice core, located on a coastal dome in east central Greenland.

The Renland peninsula is located on the eastern coast of Greenland in the Scoresbysund Fjord (Fig. 1). The ice cap is unique in that it is isolated from the Greenland Ice Sheet by steep fjords and is only 80 km wide; as a result, the thickness of the ice

https://doi.org/10.5194/cp-2020-19
Preprint. Discussion started: 24 February 2020

Climate of the Past Discussions

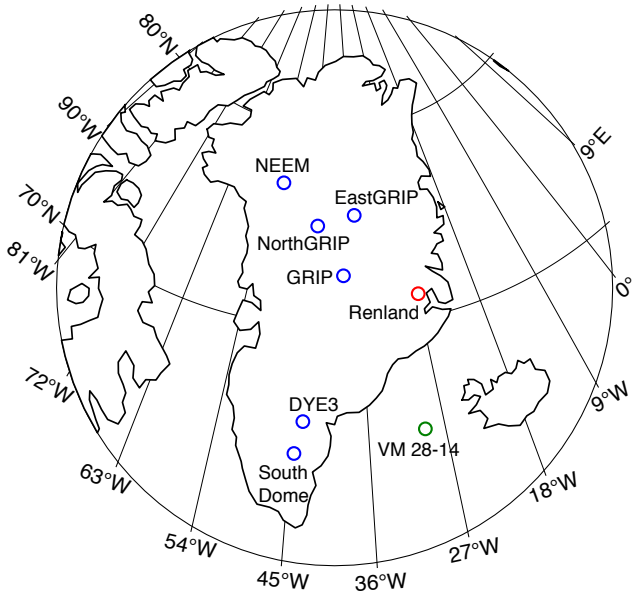

Figure 1. The Renland ice cap is located on the East coast of Greenland. The ice cap is approximately 80 km wide, and is isolated from the Greenland ice sheet. The drill site is near the summit of the ice cap, at a location of -26.75, 71.2333 (Pawlowicz, 2020).

cap is constrained and did not experience significant change during most of the Holocene (Vinther et al., 2009; Johnsen et al., 1992). The Renland peninsula experienced post-glacial uplift in the early Holocene due to ice sheet retreat, but the rate of uplift has been minimal over the last 7 ka (Vinther et al., 2009). These factors imply that the climate record is not influenced by long-term changes in elevation through the mid to late Holocene. The modern accumulation rate at Renland is approximately 45 cm ice equivalent precipitation per year, resulting in clearly defined annual layers. In comparison to inland ice core records, the local climate at the coastal Renland site is more closely linked to sea surface conditions such as sea ice cover, Nordic ocean currents, and North Atlantic climatology (Noone and Simmonds, 2004). These climate parameters are recorded in the ice core water isotope (i.e. δ^{18}O) record through changes in condensation temperature at the time of precipitation (Dansgaard, 1964; Dansgaard et al., 1973; Craig and Gordon, 1965; Merlivat and Jouzel, 1979; Jouzel and Merlivat, 1984; Jouzel et al., 1997). An ice core drilled on the Renland ice cap extends 584 m to bedrock, with the oldest ice dating 120 ka. Here we present the Holocene water isotope record (Fig. 2) and investigate drivers of climate patterns in east central Greenland through comparisons to North Atlantic sediment cores.

Sediment cores from the North Atlantic show that a ∼1500-year climate cycle occurred throughout the Holocene (Bond et al., 1997, 2001), referred to as the Bond cycle. The mechanism forcing this cycle is still under debate, but it is potentially driven by solar forcing (Bond et al., 2001) or internal climate dynamics such as interactions between the ocean and atmosphere (Wanner et al., 2015). The effects are most prominent in the Arctic, likely transmitted to lower latitudes through the Atlantic Meridional Overturning Circulation (AMOC) (Bond et al., 1997, 2001; DeMonocal et al., 2000). AMOC controls heat transport to the Arctic and can have a substantial effect on Arctic climate over long timescales. Heat is supplied to the Arctic via the

https://doi.org/10.5194/cp-2020-19
Preprint. Discussion started: 24 February 2020


Climate of the Past Discussions

Norwegian Current, carrying warm Atlantic water to the Arctic (Polyakov et al., 2004); changes in heat supply and Northward advection will influence atmosphere-ocean heat exchange, regional Arctic climate, and sea ice cover (Muilwijk et al., 2018).

The modern instrumental record documents a number of influences on higher frequency climate variability in the North Atlantic. Heat distribution through AMOC controls sea surface temperature and drives the Atlantic Multidecadal Oscillation (AMO), a 20-year cycle which is observed in prior Greenland ice cores and influences sea ice cover in the Arctic (Chylek et al., 2011). Subdecadal climate cycles are also observed in the Arctic, such as the North Atlantic Oscillation (NAO), which is currently expressed in a cycle of shifting sea-level pressure differences between the Subtropical High and Subpolar Low. This multi-year cycle influences temperature, precipitation, sea ice distribution, and ocean circulation across the entire North Atlantic (Hurrell and Deser, 2009), and it is recorded in multiple proxy records including tree ring data and central- and West-Greenland ice cores (Barlow et al., 1993; Appenzeller et al., 1998).

By reconstructing a comprehensive climate record of the Holocene, we can better place modern anthropogenic climate change in context of the past. Using the water isotope record from the Renland ice core, we aim to determine the factors that influence regional North Atlantic climate evolution over the Holocene. We explore interannual- to decadal-scale oscillations in water isotopes over the last 8 ka, and investigate relationships to sediment core records in the North Atlantic. We also calculate changes in water isotope seasonality throughout the last 2.6 ka, the time period for which the annual signal can be resolved, in order to determine driving factors for summer and winter temperatures. This analysis will give insight to mechanisms which influence regional climate in coastal Greenland over several timescales.

2 Methods

2.1 Water isotope analysis

The most common form of water exists as $^{1}H_2^{16}O$, but heavy isotopologues occur in the form of $^{1}H^{2}H^{16}O$, $^{1}H_2^{18}O$, and $^{1}H_2^{17}O$ (where ^{2}H is also known as deuterium, or D). Because heavy isotopes are a very small fraction of natural water molecules, samples are measured relative to a standard (Vienna Standard Mean Ocean Water, SMOW) and are expressed in delta notation, where R is the ratio of heavy to light isotopes (ie. $^{18}O/^{16}O$ or D/H):

$$\delta = \frac{R_{sample} - R_{SMOW}}{R_{SMOW}} \times 1000 \quad (1)$$

Such that $\delta^{18}O$, δD, and $\delta^{17}O$ are expressed in parts per thousand (per mille or ‰). The water isotope record for the 584 m Renland ice core was measured using a Continuous Flow Analysis (CFA) system (Gkinis et al., 2011; Jones et al., 2017b) at the Center for Ice and Climate at the University of Copenhagen. A stick of ice is continuously melted at a rate of 2-4 cm/min, and meltwater is collected and analyzed using cavity ring-down spectrometers, a Picarro L2140-i and an L2130-i running in parallel. This technique produces $\delta^{18}O$, δD, and $\delta^{17}O$ water isotope data with sub-mm nominal resolution, due to a small amount of mixing introduced in the system. High-frequency data is then bin-averaged into 0.5 cm data points. We focus on the $\delta^{18}O$ record in this paper. Small gaps in data, inherent to the CFA methodology due to breaks in ice and transitions from

https://doi.org/10.5194/cp-2020-19
Preprint. Discussion started: 24 February 2020

Climate of the Past Discussions
Open Access
EGU

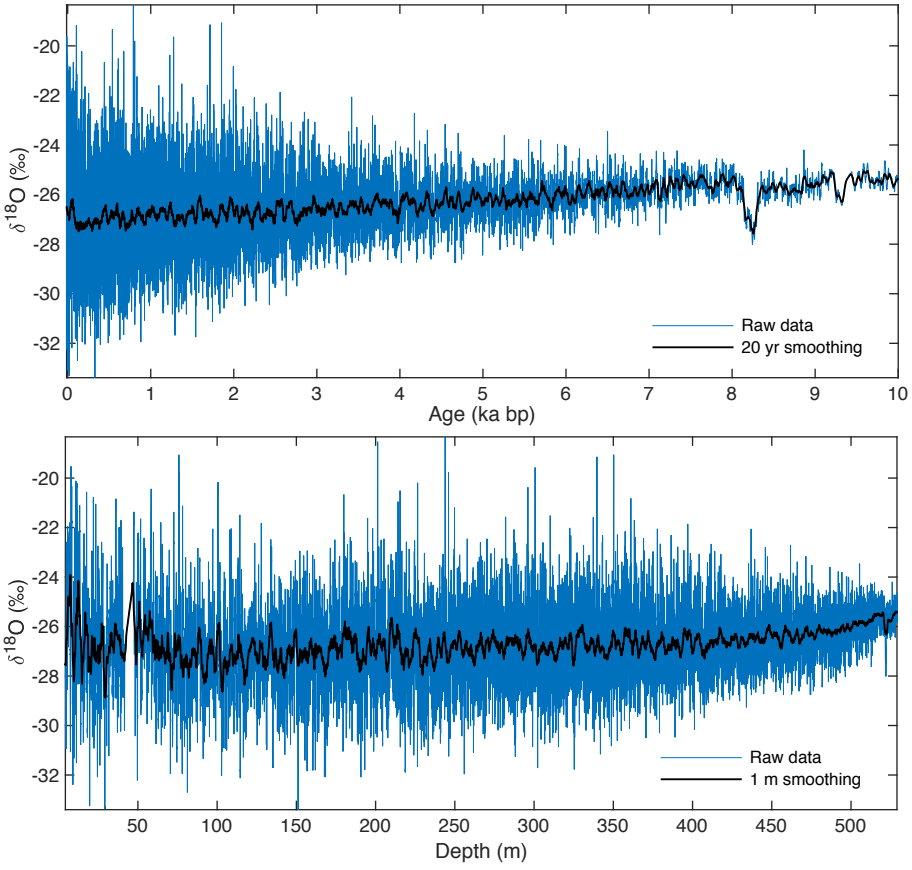

Figure 2. (Top) Holocene RECAP δ^{18}O data in time (raw, blue; 20 yr smoothing, black); and (Bottom) RECAP δ^{18}O data in depth (raw, blue; 1 m smoothing, black). The loss of high frequency data is visually observed in the shape of the δ^{18}O record, which tapers rapidly as the signal is diffused. At a depth of 529 m, the age of the ice is 10 ka.

standards (Jones et al., 2017b), are infilled using a maximum entropy method spectral technique (Andersen, 1974; Fahlman and Ulrych, 1982).

The depth-age scale for the Renland ice core is determined by Simonsen et al. (2019). For the period from 0-4035 yr bp, the StratiCounter algorithm of annual layer counting was applied (Winstrup et al., 2012; Winstrup, 2016). For ages greater than 4035 yr bp, a shape-preserving piecewise cubic interpolation is used based on Greenland Ice Core Chronology 2005 (GICC05) reference tie points (Simonsen et al., 2019). The full time scale is also fit to a series of tie points using the GICC05 reference timescale (Simonsen et al., 2019).

The Renland record exhibits much higher resolution in the Holocene because high-frequency variability is lost rapidly with depth. This occurs for two reasons: 1) At the last glacial maximum, the Laurentide ice sheet extended to approximately 40° N, and the associated temperature decrease and sea ice increase led to significantly drier conditions with minimal precipitation in Greenland. As a result, water isotope diffusion has a much greater effect in glacial ice, acting to eliminate high frequency

https://doi.org/10.5194/cp-2020-19
Preprint. Discussion started: 24 February 2020


Climate of the Past Discussions

signals. 2) Extreme basal thinning (see Fig. B1) effectively deforms annual layers into very thin intervals of ice, allowing solid-phase water isotope diffusion to have a disproportionately strong effect on the oldest ice. The glacial period is condensed into approximately 30 m, and no high-frequency climate signals (i.e. annual, interannual, decadal) are preserved. As a result, we focus here on the Holocene record through 10 ka, which has retained greater high-frequency climate information.

2.2 Vapor diffusion

In addition to climate variability, post-depositional processes affect the water isotope signal recorded in an ice core. The upper layers of the ice sheet are known as the firn column, in which the snow grains remain unconsolidated and open interconnected pathways between pore spaces allow for vapor transport. As vapor diffuses in the firn column along concentration, temperature, and vapor-pressure gradients, exchange of water molecules takes place between snow grains and vapor. This process, known as firn diffusion, attenuates the seasonal water isotope signal, acting as a smoothing function (Whillans and Grootes, 1985; Cuffey and Steig, 1998; Johnsen et al., 2000; Jones et al., 2017a). Solid-phase water isotope diffusion in ice below the firn column occurs at a much slower rate, but over thousands of years can still have a substantial impact on the attenuation and smoothing of high frequency signals. For the deeper layers closer to bedrock, solid ice diffusivities increase exponentially as the ice becomes warmer. (Itagaki, 1967; Robin, 1983; Johnsen et al., 2000; Gkinis et al., 2014; Jones et al., 2017a).

At the pore close-off density of 804.3 kg/m^3 (Johnsen et al., 2000; Jean-Baptiste et al., 1998), the transition between firn and ice occurs. The age of the ice at which this occurs is influenced by accumulation rate and temperature, and at Renland is 76 yr bp (56 m below surface). All following calculations do not include the period 0-76 yr bp, because the extent of diffusion varies substantially in this interval.

The extent of diffusion is characterized by the diffusion length parameter σ_z (units meters), which represents the mean displacement of water molecules from their relative original position (Johnsen et al., 2000; Gkinis et al., 2014; Holme et al., 2019; Jones et al., 2017a). Spectral analysis is used to estimate the diffusion length, including effects of firn diffusion, solid-phase diffusion, and CFA system mixing. The Multi Taper Method (MTM) of Fourier transform is applied to sections of the water isotope record in depth domain (i.e. 0.5 cm resolution), using overlapping windows corresponding to 300-year time periods with a 100-year time step. This produces a spectrum of power density (PD) ($‰^2$m) vs. frequency (f) (cycles/m). Vapor diffusion in the firn column causes the power density to progressively decrease at higher frequencies, taking the form of quasi-red noise. To estimate diffusion length, we apply the following methods described in Jones et al. (2017a); Kahle et al. (2018), and Holme et al. (2019). The power density spectrum of the ice core data can be described by an exponential decay model assuming Gaussian measurement noise:

$$P(f) = P_0(f) \cdot exp(-(2\pi f \sigma_z)^2) + N(f) \quad (2)$$

Where $P(f)$ is the diffused power density spectrum derived from the raw water isotope data, $P_0(f)$ is the signal prior to diffusion, and $N(f)$ is measurement noise. Eq. 2 is fit to the diffused portion of the power density spectrum to estimate σ_z (Fig. 3a).

https://doi.org/10.5194/cp-2020-19
Preprint. Discussion started: 24 February 2020


Climate of the Past Discussions

To estimate the uncertainty range for σ_z, a linear regression is calculated for ln(PD) vs f^2 of the diffused section of data (Fig. 3b). We find the maximum and minimum slope (m_{lr}) within one standard deviation of the linear fit:

$$\hat{\sigma_z} = \frac{1}{2\pi\sqrt{2}} \cdot \left(\frac{1}{2|m_{lr}|}\right)^{-\frac{1}{2}} \tag{3}$$

Where $\hat{\sigma}_z$ represents one standard deviation of the diffusion length.

Improvements to the fitting routine have been made to account for a higher density of data points at high frequency, which biases the fit of the Gaussian to high frequencies. The data is binned and averaged evenly in log-space frequency, and the Gaussian is fit to averaged data points using a least-squares optimization. Finally, the diffusion length in meters is converted to time using the following equation:

$$\sigma_t = \frac{\sigma_z}{\lambda_{avg}} \tag{4}$$

Where λ_{avg} is the mean annual layer thickness (m/yr) for the given window. The diffusion length in the depth domain (Fig. 3c) rapidly decreases with the age of ice, because the deeper layers of the Renland ice cap are subject to extreme thinning. As ice layers are buried and compacted, water molecules which were dispersed in the firn via vapor diffusion are brought closer towards their original relative position in the ice due to thinning. The diffusion length in the time domain (Fig. 3d) increases with age, potentially due to effects of solid-phase diffusion. Alternatively, changes in surface conditions (i.e. temperature, accumulation rate, air pressure), could have influenced the extent of firn diffusion at the time of deposition (Whillans and Grootes, 1985; Johnsen et al., 2000).

Reliable diffusion length estimation can be applied to water isotope data over the range ~0.1-8 ka. However, there are two problematic sections from 5.6-6.7 and 7.8-8 ka, in which the power spectral model fails to accurately describe the power spectral densities (Kahle et al., 2018), adding uncertainty to the diffusion length estimation. We compare two fitting routines for all spectra from 5.6-8 ka, hereafter referred to as Fit 1 and Fit 2 (see Fig. B2 for examples and further explanation of fits). As demonstrated in Fig. 3, the different fitting scenarios produce a minimal change in the diffusion length estimate. Even so, both fitting scenarios are used in all diffusion correction calculations in this paper, in order to ensure that results are not influenced by bias in the diffusion length estimate.

2.3 Signal decay of individual frequencies

Further analysis of the power density spectrum can be used to determine the amplitude of climate signals on an interannual to decadal scale. The amplitude (i.e. the strength) of individual frequencies from 1-20 years are identified for each 300-year window, as well as the frequency bands of 3-7, 7-15, 15-20, and 20-30 years. In our analysis, individual frequencies are normalized to the strength of the annual signal in the most recent window, and each frequency band is normalized to its most recent value.

The pre-diffusion strength of each frequency band is estimated from Eq. 2, with the correction carried out using diffusion lengths calculated by both Fit 1 and Fit 2. Due to uncertainty in the diffusion length estimation, the 3-7 and 7-15 year bands

https://doi.org/10.5194/cp-2020-19
Preprint. Discussion started: 24 February 2020

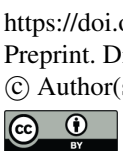

Climate of the Past Discussions
Open Access
EGU

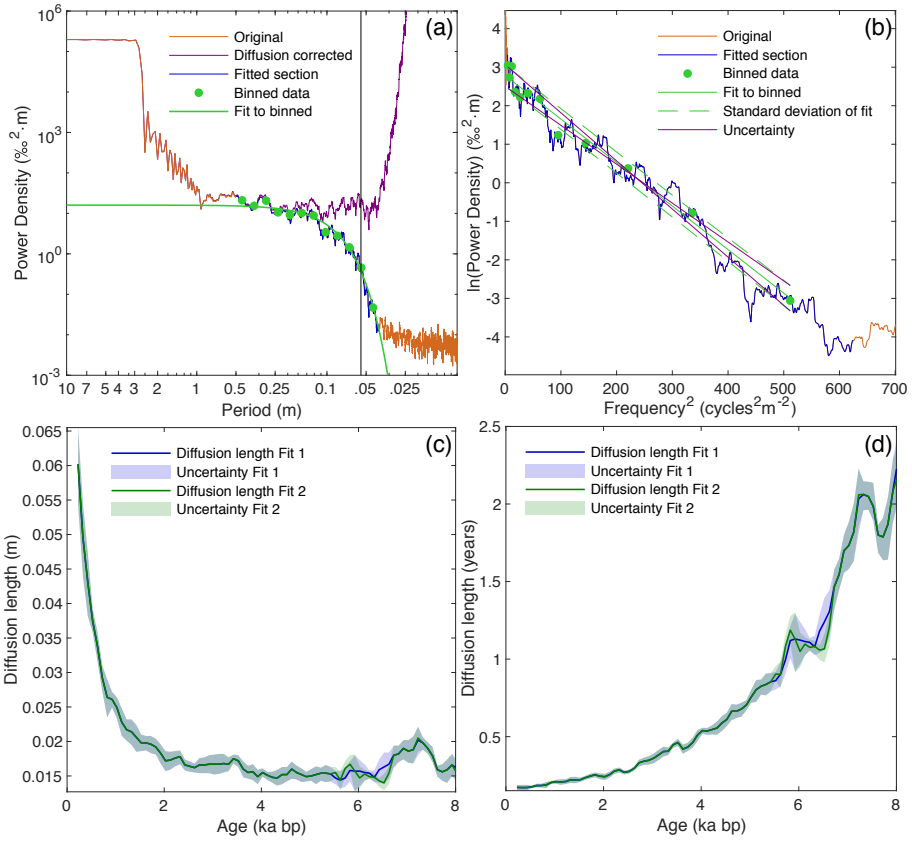

Figure 3. (a) The power density spectrum for a 300-year window from 2276-2576 yr bp. The diffused section of the spectrum is fit with a Gaussian (Eq. 2), used to estimate diffusion length for each window. The signal is cut off below a frequency of 1.1 yr^{-1} (indicated by vertical black line), after which point it is primarily noise. (b) Natural log of the same power density spectrum, used to estimate uncertainty. (c) Diffusion length estimated in depth and (d) converted to time. In both diffusion length figures, the two fitting scenarios and their respective uncertainty is designated by blue (Fit 1) and green (Fit 2). The section from 5.6-6.7 ka has the lowest quality spectra, resulting in a small difference in the diffusion length estimates.

can be corrected for diffusion over the range ∼0.1-5.5 ka; over this time period uncertainty is better constrained. The decadal bands (15-20 and 20-30 years) are substantially less affected by diffusion and can be corrected from ∼0.1-8 ka.

2.4 Deconvolution and identification of seasonal signal

Deconvolution is used to correct for the effects of diffusion on the original water isotope signal as it existed at the surface of the ice sheet, including effects of firn diffusion, solid-phase diffusion, and CFA system mixing (Johnsen et al., 2000; Vinther et al., 2003). An estimate of the original power spectrum (i.e. P_0', where P_0 is the original power spectrum prior to diffusion, and P_0' is our estimate of it) is obtained by using the diffusion length estimates for each 300-year window, producing a diffusion

https://doi.org/10.5194/cp-2020-19
Preprint. Discussion started: 24 February 2020

Climate of the Past Discussions
Open Access
EGU

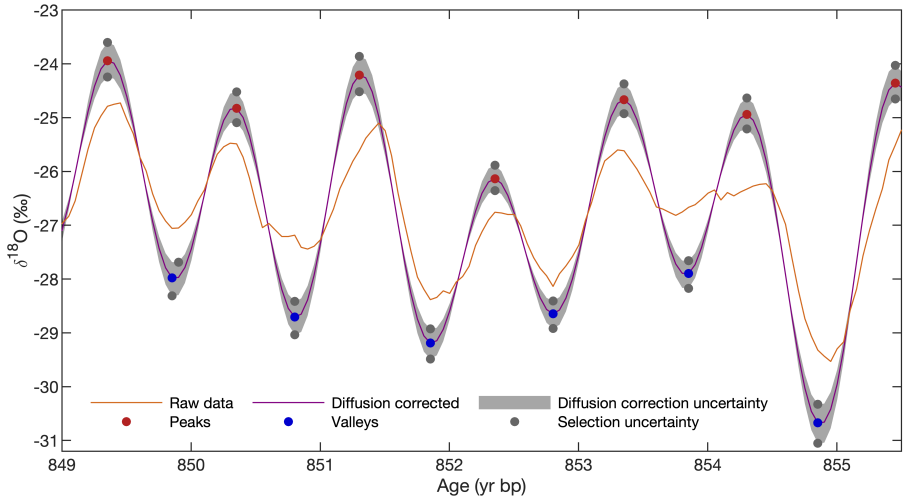

Figure 4. An example of diffusion corrected data, with summer maximum (red) and winter minimum (blue) selected for each annual signal. Gray shading and points indicate uncertainty.

corrected power spectrum with noise removed below a cut-off frequency of 1.1 yr^{-1} (as demonstrated in Fig. 3a); therefore, we can assume that the term $N(f)$ in Eq. 2 is insignificant for the frequencies below the cut-off and is equal to zero. The corrected noise-free power density spectrum is then inverted to the time domain to approximate the deconvolved δ^{18}O record for each window (Vinther et al., 2003). A comparison between the raw data and the diffusion corrected signal from 76-2600 yr bp is shown in Fig. 9. The diffusion correction is also carried out using diffusion length uncertainty values (Fig. 4).

A peak detection algorithm (built-in Matlab function findpeaks) is used to select extrema (summer and winters) in the deconvolved δ^{18}O signal from 76-2600 yr bp (Fig. 4). A 40-year moving average is applied to filter out high frequency noise and distinguish long-term trends (Fig. 9).

2.5 Community Firn Model

We use the Community Firn Model (CFM) (Stevens et al., 2020) to test five 490-year scenarios for isotope evolution, based upon temperature and accumulation fields from 1958-1978 provided by the Modèle Atmosphérique Régional (MAR; version 3.9 with monthly ERA forcing) (Fettweis et al., 2017) and a constant amplitude (4‰) sine wave to represent the annual isotopic variability (Fig. 5). For the 20-year period (Fig. B3), MAR predicts that the summer months July-September receive the most precipitation on average. The mean monthly 1958-1978 temperature cycle from MAR is used for all scenarios, while the following variations on the seasonality of accumulation are used: (1) 'Constant': Constant values for monthly accumulation rate (i.e. each month receives the same amount of accumulation); (2) 'Cycle': Repeating annual cycle, with each month's precipitation value assigned the 20-year mean accumulation rate from MAR for that month (as shown in Fig. 5); (3) 'Noise': As in (2), but with noise added to the cycled values; the statistics of the noise are derived from the standard deviation of the

https://doi.org/10.5194/cp-2020-19
Preprint. Discussion started: 24 February 2020

Climate of the Past Discussions
Open Access
EGU

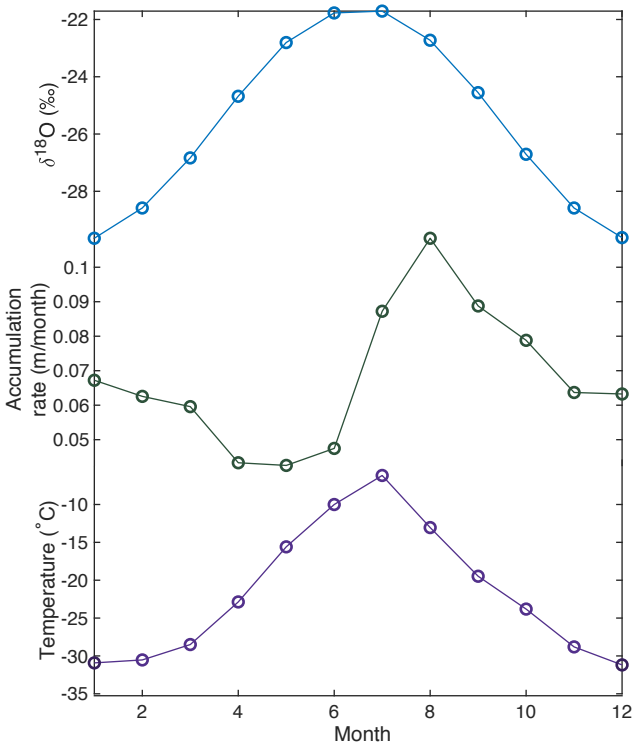

Figure 5. CFM input based on the 20 year period of MAR data from 1958-1978. (Top) Starting isotope data, based on the seasonal isotope signal observed at the top of the Renland core; (Middle) Mean monthly accumulation rate from MAR; and (Bottom) Mean monthly temperature based on the MAR data. Renland experiences a slight bias for summer accumulation, with the months July-September receiving the most accumulation.

20-year MAR time series for each month; (4) 'Random': Random value selected from the normal distribution of each month's 20-year MAR time series; and (5) 'Loop': Repeating (looped) 20-year intervals of MAR data.

The temperature, accumulation, and synthetic isotope data are input to the CFM to produce an estimate of how the isotopic signal is diffused within the firn column over a 490-year period. The resulting water isotope record represents the effects of
175 firn densification (Kuipers Munneke et al., 2015), vapor diffusion (Johnsen et al., 2000), and climate conditions on an ice core water isotope record. In our analysis, the diffused isotope signal from 390-490 years is selected, because this is below the bubble close off depth of the firn column. As with the observed ice core data, we diffusion correct the model data, and select the summer and winter extrema values.

https://doi.org/10.5194/cp-2020-19
Preprint. Discussion started: 24 February 2020

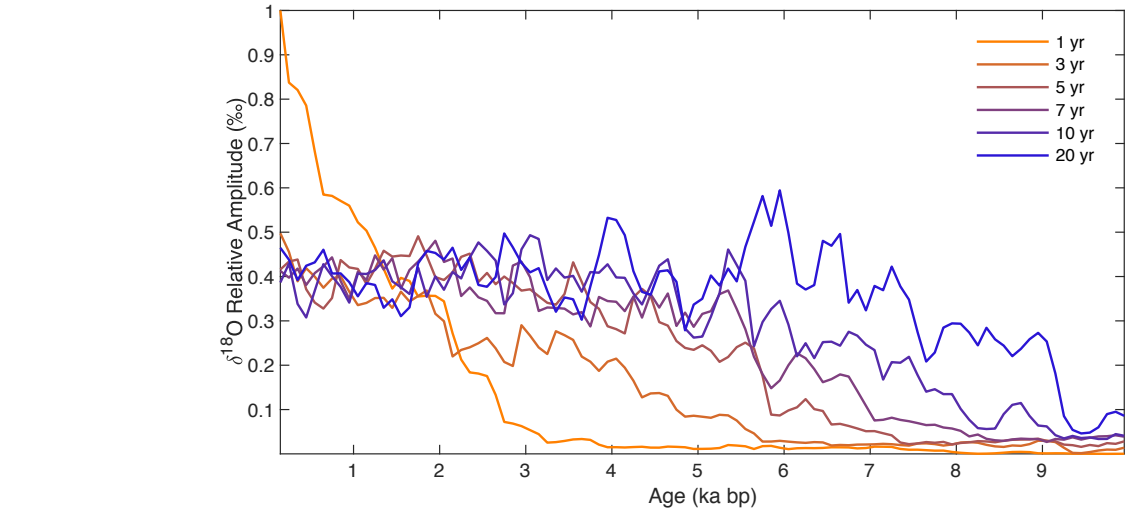

Figure 6. Individual frequency bands demonstrate how rapidly the annual signal dissipates, while lower frequency signals are preserved for a greater period of time. All bands are normalized to the strength of the annual frequency in the most recent window.

3 Results and discussion

3.1 Interannual climate variability

The strength of the annual signal in δ^{18}O decays rapidly due to diffusion (Fig. 6), but persists to approximately 2.6 ka. After this time, the annual signal cannot be diffusion corrected or interpreted. The strength of interannual signals also decreases with time; for example, the 3-year signal is lost as it decays below a relative amplitude of 0.05‰ at ∼5.6 ka and the 5-year signal is lost at ∼7 ka. The decadal signal is preserved for most of the Holocene, extending to about 8 ka (Fig. 6). Further analysis of frequency bands (3-7, 7-15, 15-20, 20-30 year bands) is also used to investigate variability of interannual and decadal climate signals (Fig. 7) (Jones et al., 2018). Each frequency band is diffusion corrected and normalized to its value in the most recent time window. The higher frequency bands are more diffused, and we find that the 3-7 and 7-15 year bands are not reliably corrected after 5.5 ka due to uncertainty in the diffusion length estimate (see Fig. 3).

After an investigation of how frequency bands compare to other climate records, we find the 15-20 year band has distinct similarities to a record of hematite-stained grains (HSG) in North Atlantic sediment core VM 28-14 (Bond et al., 2001) (Fig. 1, Fig. 8). The full span of the two records has a correlation coefficient $r = 0.34$, while the period from 2.5-6.4 ka has a stronger relationship with $r = 0.74$. Both relationships have a p-value <0.01, indicating that they are statistically significant. While we cannot rule out the possibility that this similarity arises due to random noise in the climate system, considering the common geographic region, there are potential mechanisms that could link the two records.

Percent HSG in an ocean sediment core is sensitive to the amount and source of glacial ice and sea ice, reflecting circulation in surface ocean waters. An increase in HSG in core VM 28-14 is indicative of a greater influx of cold surface waters carrying

https://doi.org/10.5194/cp-2020-19
Preprint. Discussion started: 24 February 2020

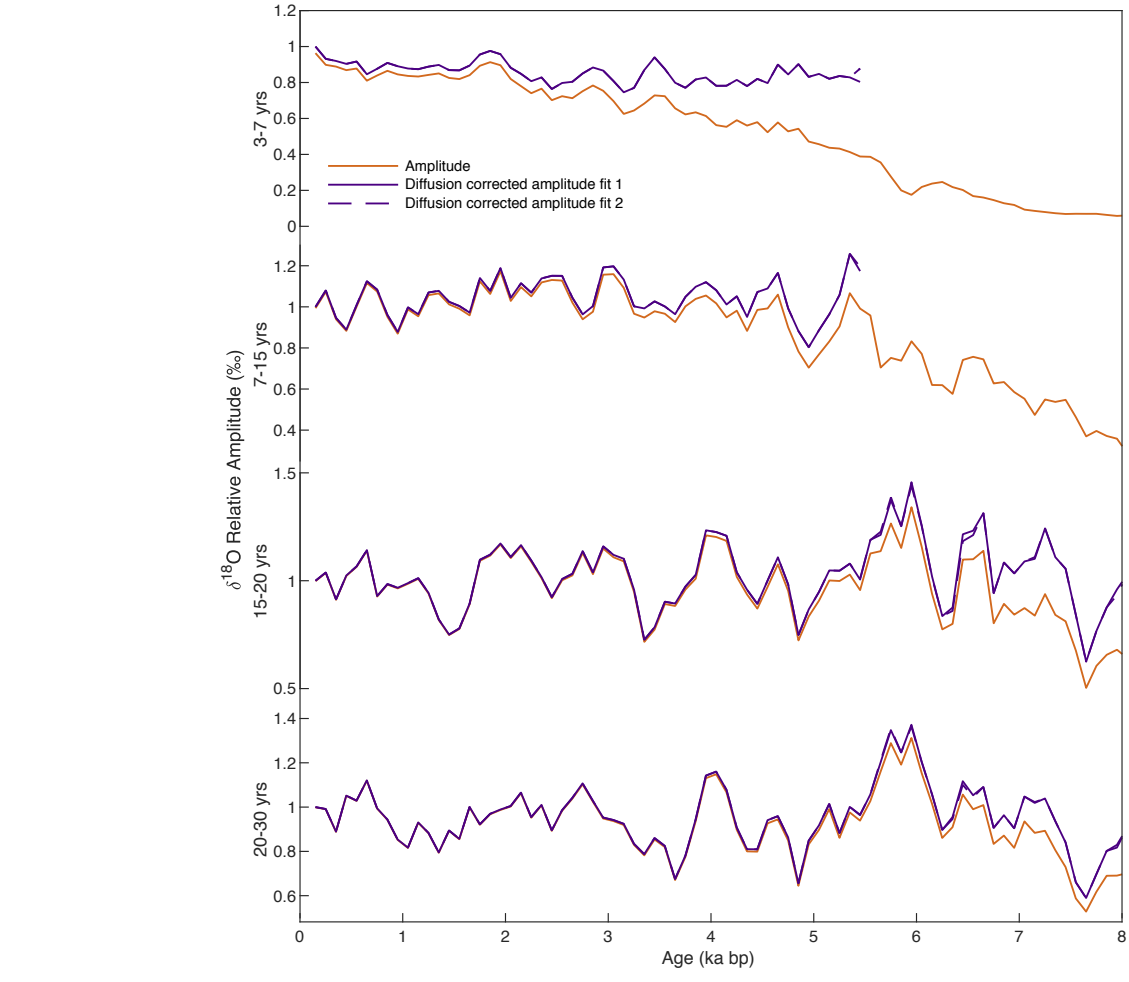

Figure 7. The normalized relative amplitude for 3-7, 7-15, 15-20, and 20-30 year bands (orange) decreases with time due to diffusion and thinning in the ice core. The solid and dashed purple lines indicate the diffusion corrected relative amplitude, using two different fitting scenarios for the diffusion length estimate. Each band is normalized to the amplitude of the respective diffusion corrected signal in the most recent window. The diffusion correction of frequency bands 3-7 and 7-15 years is cut off at 5.5 ka due to uncertainties in the diffusion length. Decadal bands from 15-20 and 20-30 years are not as affected by diffusion, and are corrected through 8 ka. The point at which the diffusion correction deviates from the original value shows that as the frequency decreases, the signal resists attenuation for a greater period of time.

drift ice from the Nordic seas, driven by strong northerly winds (Bond et al., 2001; Andrews et al., 2014). Millennial variability observed in VM 28-14 occurs with a 1500-year periodicity, known as Bond events. The mechanism driving these events has long been a source of debate. A comparison with Beryllium records in Greenland ice cores and carbon-14 in tree rings shows
200 that increases in drift ice and HSG correspond to intervals of variable and decreased insolation (Bond et al., 2001), suggesting that changes in millennial-scale circulation are driven by insolation. However, more recent studies suggest that Bond events are unrelated to insolation and are due to internal climate system variability or volcanic activity (Wanner et al., 2015). While the

https://doi.org/10.5194/cp-2020-19
Preprint. Discussion started: 24 February 2020

Climate of the Past Discussions
Open Access
EGU

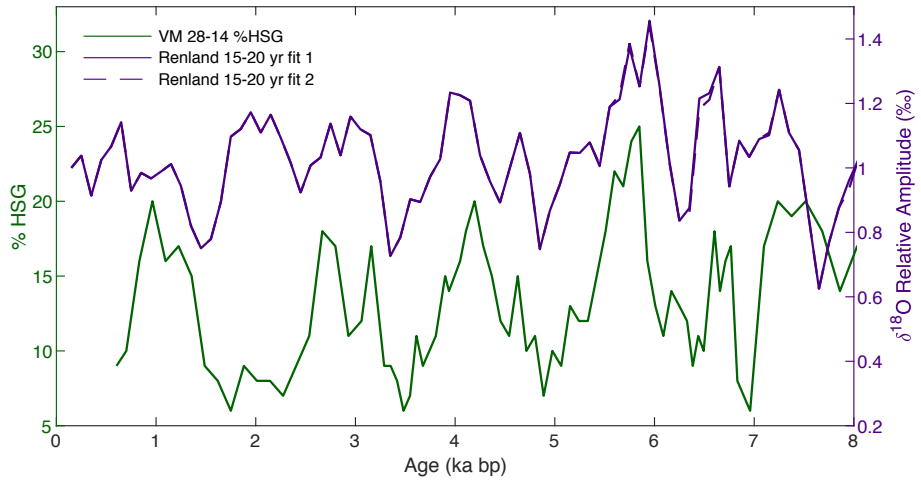

Figure 8. Comparison of %HSG from North Atlantic sediment core VM 28-14, a tracer for drift ice (Bond et al., 2001) and diffusion corrected 15-20 year relative amplitude of δ^{18}O in the Renland ice core, normalized to its starting amplitude. The period from 2.5-6.4 ka exhibits the strongest relationship, with correlation coefficient r = 0.74.

driving mechanism remains uncertain, it is known that percent HSG fluctuates with influxes of Nordic surface waters which flow along the eastern coast of Greenland and near the Renland core location (Bond et al., 2001; Andrews et al., 2014).

Modern observations of North Atlantic variability may provide some clues as to why the amplitude of the 15-20 year band has apparent similarities with regional ocean circulation. One potential climate mechanism that could be expressed in the 15-20 year δ^{18}O variability is the North Atlantic Oscillation (NAO), as fluctuations in insolation could influence the strength of the NAO through changes in sea surface temperature (Shindell et al., 2001). The NAO is observed in water isotope and accumulation records of central and west Greenland ice core records through the 19th century, but the δ^{18}O-NAO relationship on the east coast of Greenland is weak (Appenzeller et al., 1998; Barlow et al., 1993; Vinther et al., 2003, 2010).

Similarly, a recent analysis of the last 200 years of stacked ice core records from Renland demonstrated that δ^{18}O shows varying levels of weak correlation with NAO (Holme et al., 2019). Instead, the δ^{18}O signal is dominated by a combination of climate conditions including regional temperature and sea ice extent in the Fram Strait. During periods of increased sea ice extent, the δ^{18}O-temperature relationship at Renland is weaker. Similarly, the 15-20 year variability throughout the Holocene may be responding to regional temperature, sea ice extent, and how these factors are influenced by interaction with ocean circulation.

The connection between sea surface conditions and ice core records is further supported by a previous study linking water isotope variability in a stack of five Greenland ice cores to the Atlantic Multidecadal Oscillation (AMO) using instrumental and proxy records (Chylek et al., 2011). Over the period from 1303-1961, all records exhibited a similar 20-year signal. This relationship is attributed to changes in sea surface temperature (SST), driven by AMO and associated with variability in Atlantic Meridional Overturning Circulation (AMOC) in the North Atlantic basin (Chylek et al., 2011; Frankcombe et al.,

https://doi.org/10.5194/cp-2020-19
Preprint. Discussion started: 24 February 2020


Climate of the Past Discussions

2010). The SST and Arctic climate are sensitive to the strength of AMOC, as a reduction in overturning circulation would lead to decreased northward heat transport. These findings suggest that the variability in the 15-20 year δ^{18}O signal at Renland may be associated with the AMO, driven by AMOC and the associated sea surface conditions including both ice cover and SST. Additionally, Knight et al. (2005) shows that the AMO signal observed in the HadCM3 model is non-stationary on millennial time scales. While the correlation between the marine HSG record and the Renland ice core water isotope record alone may not be conclusive evidence of this relationship, there is a plausible physical connection between the Bond events and the decadal variability observed in Greenland. Additional studies that reduce timescale uncertainties in ocean sediment records, in combination with further modeling of the physical processes, would help to constrain the mechanisms linking the two records. Modeling in particular can elucidate the millennial-scale relationships between the east Greenland ice sheet, North Atlantic ocean dynamics, and regional climate patterns.

3.2 Late-Holocene seasonality

As part of the annual cycle, maximum summer and minimum winter δ^{18}O values were determined using a selection algorithm for the period from 76-2,600 years bp (Fig. 9). The winter δ^{18}O signal decreases toward present with the average modern value approximately 1.2‰ lower than the average value at 2.6 ka bp. The summer signal trend over this same time period is relatively flat. Both summer and winter records exhibit non-stationary centennial-scale variability over the last 2.6 ka. The amplitude of the annual signal (half the summer to winter difference) has increased by approximately 50% from 2.6 ka to the present, indicating stronger seasonality in the modern Arctic climate system. Here we investigate several potential mechanisms that could drive a decrease in winter δ^{18}O at Renland, and the associated amplitude increase.

3.2.1 Seasonality of accumulation

The seasonality of accumulation creates uncertainty in the diffusion correction calculation of the annual cycle. If there is a seasonal precipitation bias (i.e. more snow in summer than winter), the drier season will be subject to greater isotopic attenuation due to firn diffusion. Because we cannot selectively diffusion correct the seasonal isotope signal for accumulation bias, we must assume constant seasonality of accumulation. Therefore, the drier season will be under-corrected for diffusion, and the wetter season will be over-corrected to a lesser extent, resulting in potential inaccuracies in the amplitude of the seasonal signal. While there is no current method for reconstructing past seasonality of accumulation, we can utilize a series of tests to determine the extent to which the diffusion correction calculation for water isotopes could be affected by seasonally-biased precipitation.

We compare the diffusion corrected outputs from the Community Firn Model (CFM) when it is forced with the five accumulation scenarios (constant, cycle, noise, random, loop) described in Section 2.5. The model results show that the Renland diffusion correction is minimally influenced by seasonality of accumulation (Fig. 10). This outcome is unique to the Renland site, which has a much higher accumulation rate ($\sim$1.5 meters of snowfall per year) in comparison to other inland Greenland ice core sites (at least $\sim$50% less). In the model, all seasonally-biased accumulation scenarios exhibit an annual amplitude that is slightly under-corrected for diffusion, and is smaller than the pre-diffusion amplitude. The greatest effect occurs on winter

https://doi.org/10.5194/cp-2020-19
Preprint. Discussion started: 24 February 2020

Climate of the Past Discussions
Open Access
EGU

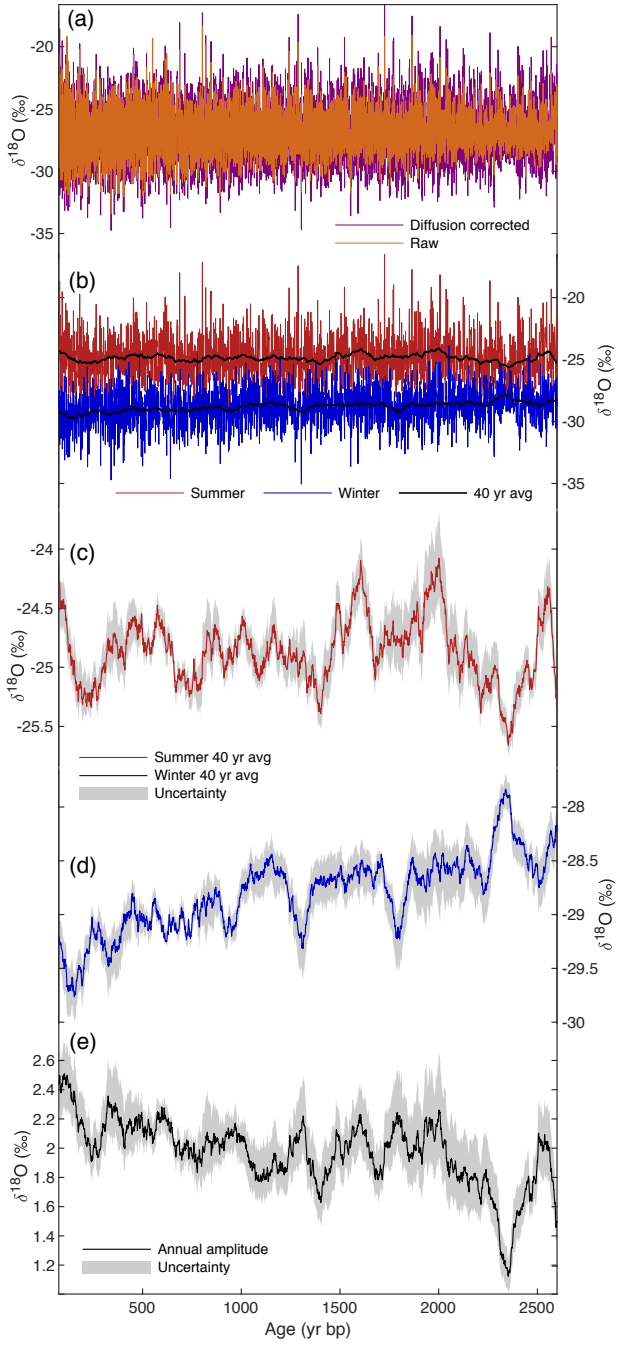

Figure 9. (a) Comparison of raw and back diffused data; (b) seasonal signal for back diffused data (summer is red; winter is blue) with a 40-year moving average applied in bold; (c,d) 40-year moving average of seasonal signal with maximum and minimum uncertainty indicated by gray shading; (e) annual amplitude of seasonal signal with maximum and minimum uncertainty indicated by gray shading.

https://doi.org/10.5194/cp-2020-19
Preprint. Discussion started: 24 February 2020

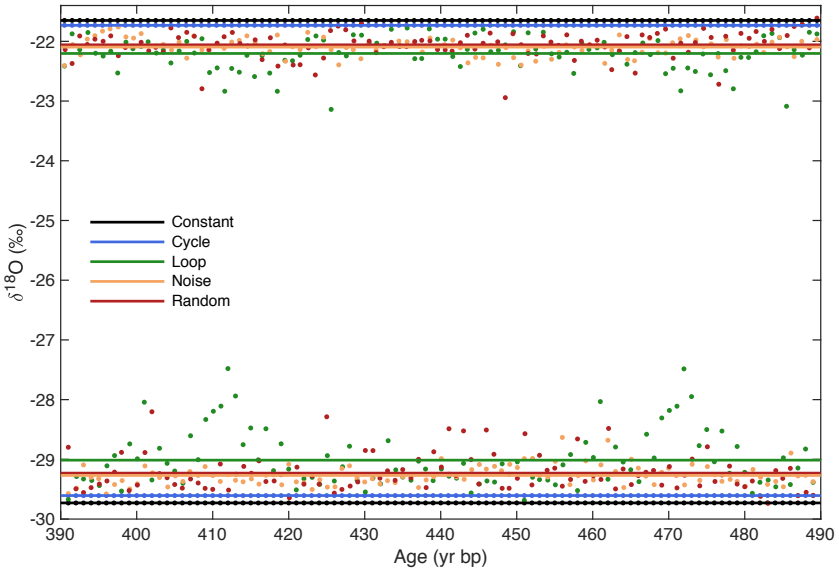

Figure 10. Comparison of seasonality for five different accumulation scenarios: constant, cycle, loop, noise, and random. Scattered points represent individual summer and winter maxima for the diffusion corrected CFM output, and solid lines represent the mean of the full 100-year window.

255 months which receive less accumulation in the MAR reanalysis. There is a maximum 18% difference in the annual amplitude of diffusion corrected isotope values between the constant and varied accumulation scenarios, which is a direct result of the bias in the diffusion correction. Thus, in the unlikely case that accumulation shifted from a constant scenario to a seasonal-bias over the last 2.6 ka at Renland, we would expect up to an 18% offset from the true value of the annual amplitude. There is no indication this would have occurred in any reanalysis or model product in which we are aware. Furthermore, the annual ampli-
260 tude in the observed Renland water isotope record increases by approximately 50% over the last 2.6 ka, which is substantially beyond what can reasonably be expected from changes in accumulation bias.

Since the Renland site is subject to warm summer temperatures, we must also consider the possible effects of melt layers on the seasonal signal. If frequent melt events caused summer melt water to percolate through the firn column, this could cause vertical mixing with the underlying winter layer. This mixing would cause a decrease in the amplitude of the signal.
265 Alternatively, melt water which refreezes in the firn as an ice lens can produce a local barrier to further diffusion. In either case, it is important to consider the extent to which melt layers could influence the recorded water isotope signal. Taranczewski et al. (2019) measured the density of melt layers at Renland, determining a high resolution record for the last 2.1 ka. The ratio of snow water equivalent of a melt layer to the respective annual layer is characterized as the annual melt ratio (AMR), which over the last 2.1 ka has an average value of less than 0.02 and is therefore a very small fraction of the total annual accumulation
270 (about 3 cm for 1.5 m snow per year). The AMR exhibited some centennial variability with a few distinct periods of increased melt, and has increased in modern times since 1860 CE. However, the melt layer data did not demonstrate a long-term trend

https://doi.org/10.5194/cp-2020-19
Preprint. Discussion started: 24 February 2020

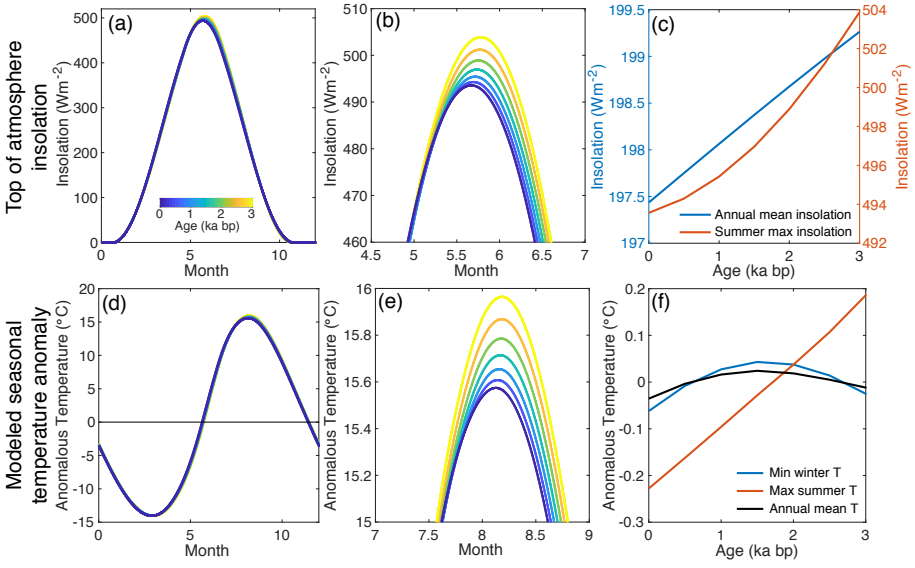

Figure 11. Changes in insolation (a-c) and expectation for temperature change (d-f) from a simple energy balance model. (a) Seasonal cycle of insolation at 71° N, colored by age (in ka bp). (b) Same as (a) but zoomed in on summer. (c) Changes in maximum summer insolation (red) and annual mean insolation (blue) at 71° N over the last 3 ka. (d) Modeled energy balance temperature anomaly at 71° N (as deviation from annual mean), colored by age (in ka bp). (e) Same as (d) but zoomed in on summer. (f) Changes in maximum summer temperature (red), minimum winter temperature (blue), and annual mean temperature (black) at 71° N.

over the last 2.6 ka (Taranczewski et al., 2019), indicating that the presence of melt layers is not influencing the seasonality trends observed in the δ^{18}O signal. Furthermore, recent increases in melt layer occurrence would likely serve to decrease the annual amplitude (which we do not observe) and the snow layers are so thick at Renland that any percolation of liquid water will have a nearly negligible effect (i.e. avg. AMR = 0.02, with avg. 1.5 m snow per year).

3.2.2 Insolation

We next consider the effects of insolation, which is expected to directly influence seasonal temperatures, and by extension the water isotopes at Renland. To the first-order, orbital parameters (i.e. eccentricity, obliquity, precession) modulate the timing and intensity of top of atmosphere (TOA) incoming radiation, and should drive peak summer temperatures and isotope values. Because Renland is located at a high latitude, the site receives minimal or no insolation throughout the winter, meaning that integrated summer insolation dominates. Thus, winter temperatures are less dependent on direct solar input, and instead are subject to the effects of lateral atmospheric heat transport and the efficiency of cooling from summer.

Here we assess the potential direct influence of changing solar insolation due to variations in the Earth's orbit on seasonal radiative equilibrium temperatures at Renland. We calculate the TOA insolation forcing at 71° N (Fig. 11a-c) (Huybers, 2011), which shows a small decline in maximum (and integrated) summer insolation over the last 3 ka, as well as a slight decline in annual mean insolation. We use a relatively simple energy balance model to calculate expected changes in seasonal surface

https://doi.org/10.5194/cp-2020-19
Preprint. Discussion started: 24 February 2020


Climate of the Past Discussions

temperature (Fig. 11d-f), that accounts for the above changes in insolation, temperature-dependent emission back to space, and horizontal atmospheric heat transport which is modeled as the diffusion of near-surface moist static energy (Hwang and Frierson, 2010). Expected peak summer temperatures decline slightly over the last 3 ka, in line with declining TOA summer insolation (Fig. 11c,f), while minimum winter temperatures remain relatively unchanged. These results are robust to a number of assumptions in the simple energy balance model. The expected seasonal temperature trends due solely to changes in insolation are not able to account for the observed changes in seasonal δ^{18}O at the Renland site.

However, there may be indirect solar effects that affect other parts of the climate system, which then exert an influence on Renland. One possibility is sea ice extent, which is both influenced by annual insolation (Müller et al., 2012) and influences total absorbed insolation at the surface due to albedo. This may explain the similarity between the winter δ^{18}O signal and total annual insolation at 71° N.

3.2.3 Comparison to sea ice records

As a possible explanation of the declining winter signal and the associated increase in amplitude toward the present, we consider changes in sea ice extent along eastern Greenland. Since Renland is closer to the coast and open ocean than other inland ice cores (see Appendix A for a comparison to central Greenland ice core GRIP), sea ice could play a more substantial role in Renland climatology (Noone and Simmonds, 2004).

We find that a number of studies have documented an increase in sea ice over the last few millennia (Müller et al., 2012; Fisher et al., 2006; Jakobsson et al., 2010; Polyak et al., 2010). The formation of sea ice primarily occurs in winter, and increasing sea ice would be correlated with decreasing regional temperatures in winter and for portions of the shoulder seasons, depending on the timing of ice formation in Fall and melt in late Spring. Increasing sea ice is therefore consistent with increasingly colder winters at Renland, whereas summers would largely be immune to sea ice response since nearby water bodies would be ice free.

Sediment core records from the Fram Strait indicate an increase in sea ice cover over the last 3 ka (Müller et al., 2012), and iodine concentrations from the Renland ice core also suggest increasing sea ice (Corella et al., 2019; Saiz-Lopez et al., 2015). A cooling trend in this time period is also observed in records of glacial expansion, ice sheet growth, and increased drift ice (Miller et al., 2010), driven by a decrease in total annual insolation. A more open ocean regime at 2.6 ka, driven by higher total annual insolation, would keep winters warmer in coastal Greenland due to ocean heat contribution to the atmosphere (Screen and Simmonds, 2010). In recent centuries prior to the Industrial Revolution, lower total annual insolation and increased sea ice would dampen the moderating effect the open ocean has on coastal winter temperatures.

4 Conclusions

The Renland ice core from east-central Greenland contains a high-resolution water- isotope record of the Holocene, with the decadal signal preserved through 8 ka. Through spectral analysis of the δ^{18}O record, we find that decadal (15-20 year) variability over the last 8 ka exhibits similarity to the millennial-scale Bond cycle recorded in nearby North Atlantic sediment

https://doi.org/10.5194/cp-2020-19
Preprint. Discussion started: 24 February 2020

core VM 28-14. This relationship, which is strongest from approximately 2.5-6.4 ka, may be associated with changes in the Atlantic Meridional Overturning Circulation which drive fluctuations in the Atlantic Multidecadal Oscillation, sea surface temperature, and sea ice cover.

The annual δ^{18}O signal is preserved through 2.6 ka, and diffusion correction reveals a cooling trend observed only in the winter signal, while the summer signal has remained relatively stable. The resulting increase in the annual amplitude does not appear to be an artifact of seasonality of precipitation or melt layers. We instead find that the winter cooling trend is likely associated with an increase in sea ice, which is driven by a decrease in total annual insolation.

In contrast to inland Greenland ice cores, the coastal proximity of Renland makes the isotope record more subject to influence from sea surface conditions. While additional research is needed to better constrain the effects of sea ice and ocean circulation on the Renland δ^{18}O signal, this is a valuable demonstration of the additional regional climate information contained in coastal ice cores. The reversal in sea ice extent due to anthropogenic climate change will work to reverse the trend in winter cooling in coastal East Greenland over the last 2.6 ka. This is an important factor in modern Arctic climate, as retreating sea ice cover may contribute to a warming feedback loop for winter climate, that can either cause additional ice sheet melt or possibly additional winter precipitation due to a warmer atmosphere. Which effect dominates should be investigated with regional and global circulation models.

Data availability. Holocene δ^{18}O data through 8 ka will be made available at http://www.iceandclimate.nbi.ku.dk/data/. Additionally, the δ^{18}O record through 2 ka, including raw, back diffused, and peak detection results, will be submitted to the Iso2k database for public use in further analysis.

Appendix A: Comparison to the GRIP ice core

We compare the seasonality at Renland to that of GRIP (using the same methodology, see section 2). GRIP is located in central Greenland and was drilled in 1992 (Anklin et al., 1993; Johnsen et al., 1997) using discrete 2.5 cm sampling resolution. The winter signal at GRIP experiences a decreasing trend similar to Renland, while the summer signal remains stable. This results in a slight increase in the annual amplitude at GRIP over the last 3.5 ka, although the magnitude of change is more muted compared to Renland. A caveat in analyzing this data is that accumulation may have a greater seasonal bias at GRIP, and because there is less total annual accumulation this could have a greater effect on the ability to correctly back diffuse the raw data. Thus, the GRIP data should only be used as a comparison.

https://doi.org/10.5194/cp-2020-19
Preprint. Discussion started: 24 February 2020

Climate of the Past Discussions
Open Access
EGU

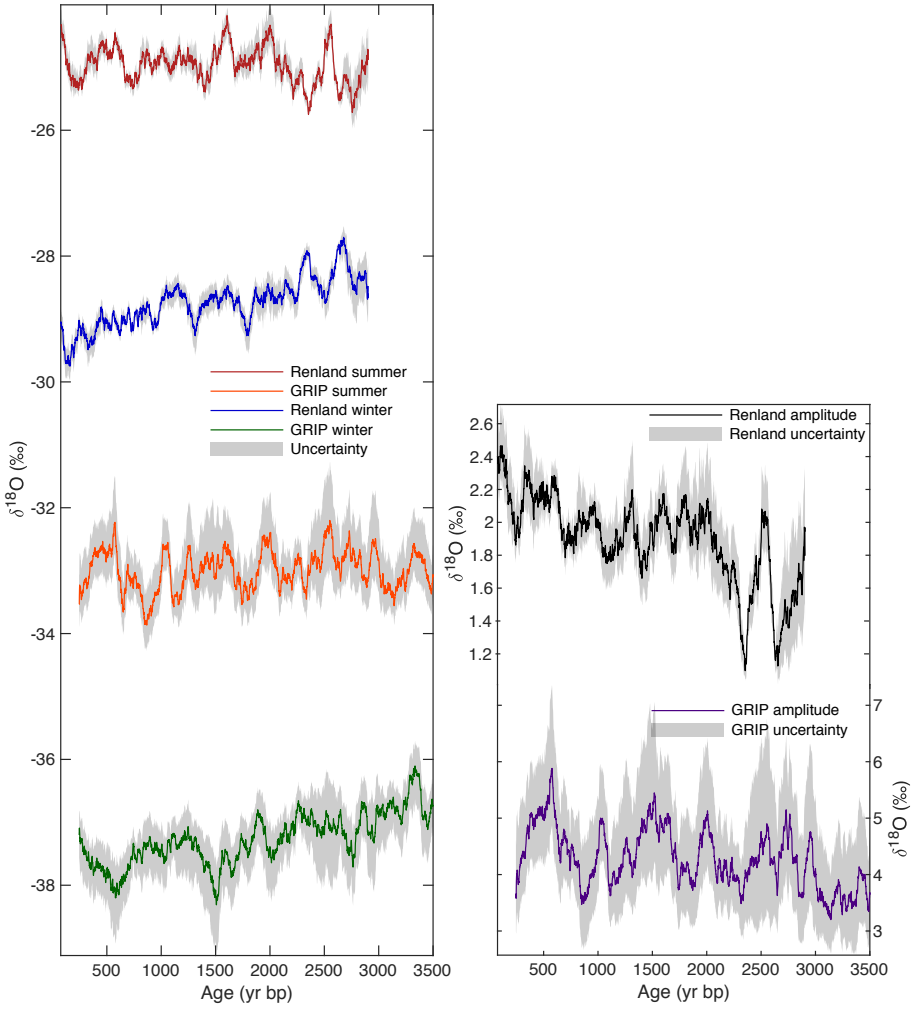

Figure A1. A comparison of Renland and GRIP seasonal data shows that GRIP experiences a similar winter cooling trend while summer is stable, resulting in a slight increase in annual amplitude at GRIP. However, the effect is muted in comparison to the trend at Renland.

https://doi.org/10.5194/cp-2020-19
Preprint. Discussion started: 24 February 2020

Climate of the Past Discussions
Open Access
EGU

Appendix B: Figures

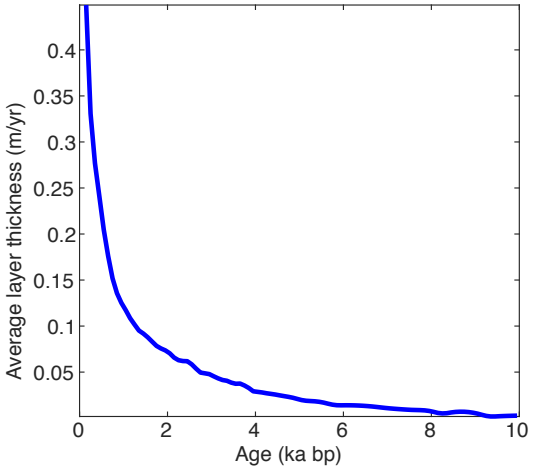

Figure B1. Mean annual layer thickness throughout the Holocene; the ice cap is rapidly thinned over the last 2 ka.

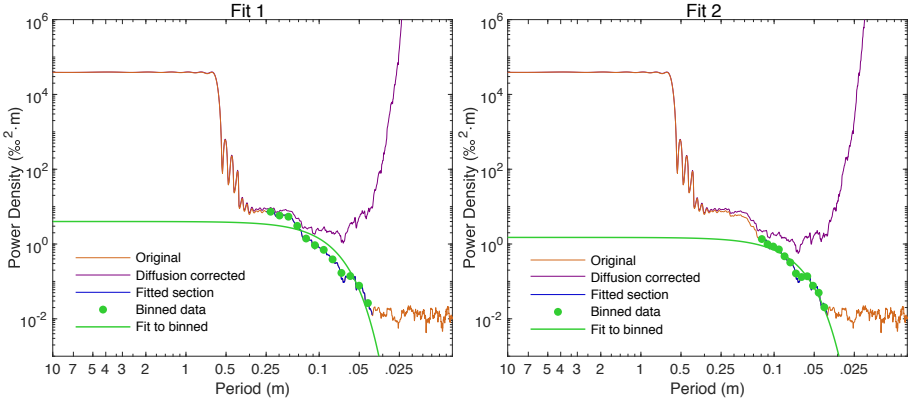

Figure B2. Example of fits to power density spectra using different fitting schemes. Left demonstrates Fit 1, in which we utilize a similar fitting range as surrounding windows to determine a diffusion. Right demonstrates Fit 2, in which the fitting range is selected so that the second Gaussian is used to determine the diffusion length.

https://doi.org/10.5194/cp-2020-19
Preprint. Discussion started: 24 February 2020

Climate of the Past Discussions
Open Access
EGU

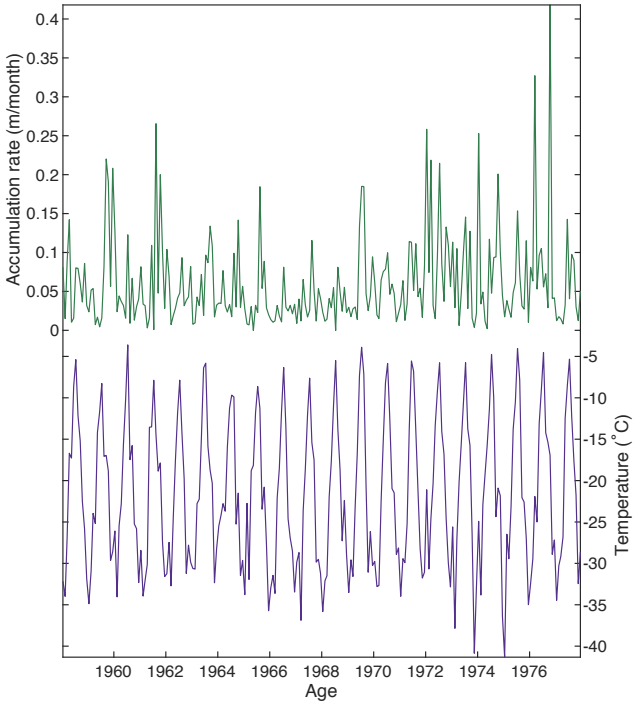

Figure B3. Monthly ice accumulation rate (top) and temperature (bottom) data for the 20-year period of MAR data from 1958-1978. The monthly averages for temperature and accumulation used for CFM input are obtained from this period.

Author contributions. AH and TRJ contributed to all aspects of this paper. AH, TRJ, VG, BMV, VM, BHV, and CH contributed to processing of the Renland ice core data. BMV developed diffusion correction code, adapted by TRJ for this study. CS provided Community Firn Model output. BM provided insolation modeling. TRJ, AH, and JW developed and implemented analysis techniques. TRJ developed the extrema (summer, winter) picking algorithm. AH wrote the manuscript with significant editorial contributions from TRJ and comments from all authors.

Competing interests. The authors declare that they have no conflict of interest.

Acknowledgements. The RECAP ice coring effort was financed by the Danish Research Council through a Sapere Aude grant, the NSF through the Division of Polar Programs, the Alfred Wegener Institute, and the European Research Council under the European Community?s Seventh Framework Programme (FP7/2007-2013)/through the Ice2Ice project and the Early Human Impact project (267696). The authors acknowledge the support of the Danish National Research Foundation through the Centre for Ice and Climate at the Niels Bohr Institute (Copenhagen, Denmark). Abigail Hughes also acknowledges support from the NSF through the Graduate Research Fellowship Program.

https://doi.org/10.5194/cp-2020-19
Preprint. Discussion started: 24 February 2020

Climate of the Past Discussions

References

Andersen, N.: On the calculation of filter coefficients for maximum entropy spectral analysys, Geophysics, 39, 69–72, 1974.

Andrews, J. T., Bigg, G. R., and Wilton, D. J.: Holocene ice-rafting and sediment transport from the glaciated margin of East Greenland (67-70°N) to the N Iceland shelves: detecting and modelling changing sediment sources, Quaternary Science Reviews, 91, 204–217, https://doi.org/10.1016/j.quascirev.2013.08.019, http://dx.doi.org/10.1016/j.quascirev.2013.08.019, 2014.

Anklin, M., Barnola, J. M., Beer, J., Blunier, T., Chappellaz, J., Clausen, H. B., Dahl-Jensen, D., Dansgaard, W., De Angelis, M., Delmas, R. J., Duval, P., Fratta, M., Fuchs, A., Fuhrer, K., Gundestrup, N., Hammer, C., Iversen, P., Johnsen, S., Jouzel, J., Kipfstuhl, J., Legrand, M., Lorius, C., Maggi, V., Miller, H., Moore, J. C., Oeschger, H., Orombelli, G., Peel, D. A., Raisbeck, G., Raynaud, D., Schott-Hvidberg, C., Schwander, J., Shoji, H., Souchez, R., Stauffer, B., Steffensen, J. P., Stievenard, M., Sveinbjornsdottir, A., Thorsteinsson, T., and Wolff, E. W.: Climate instability during the last interglacial period recorded in the GRIP ice core, Nature, 364, 203–207, https://doi.org/doi.org/10.1038/364203a0, 1993.

Appenzeller, C., Stocker, T. F., and Anklin, M.: North Atlantic Oscillation Dynamics Recorded in Greenland Ice Cores, Science, 282, 446–449, 1998.

Barlow, L. K., White, J. W. C., Barry, R. G., Rogers, J. C., and Grootes, P. M.: The North Atlantic Oscillation Signature in Deuterium and Deuterium Excess Signals in the Greenland Ice Sheet Project 2 Ice Core, 1840-1970, Geophysical Research Letters, 20, 2901–2904, 1993.

Bond, G., Showers, W., Cheseby, M., Lotti, R., Almasi, P., DeMonacal, P., Priore, P., Cullen, H., Hajdas, I., and Bonani, G.: A Pervasive Millennial-Scale Cycle in North Atlantic Holocene and Glacial Climates, Science, 278, 1257–1266, 1997.

Bond, G., Kromer, B., Beer, J., Muscheler, R., Evans, M. N., Showers, W., Hoffmann, S., Lotti-bond, R., Hajdas, I., and Bonani, G.: Persistent Solar Influence on North Atlantic Climate During the Holocene, Science, 294, 2130–2136, 2001.

Chylek, P., Folland, C. K., Dijkstra, H. A., Lesins, G., and Dubey, M. K.: Ice-core data evidence for a prominent near 20 year time-scale of the Atlantic Multidecadal Oscillation, Geophysical Research Letters, 38, 1–5, https://doi.org/10.1029/2011GL047501, 2011.

Corella, J. P., Maffezzoli, N., Cuevas, C. A., Vallelonga, P., Spolaor, A., Cozzi, G., Müller, J., Vinther, B., Barbante, C., Kjaer, H. A., Edwards, R., and Saiz-Lopez, A.: Holocene atmospheric iodine evolution over the North Atlantic, Climate of the Past Discussions, pp. 1–15, https://doi.org/10.5194/cp-2019-71, 2019.

Craig, H. and Gordon, L. I.: Deuterium and oxygen 18 variations in the ocean and the marine atmosphere, in: Stable Isotopes in Oceanographic Studies and Paleotemperatures, edited by Tongiorgi, pp. 9–130, Spoleto, 1965.

Cuffey, K. M. and Steig, E. J.: Isotopic diffusion in polar firn: implications for interpretation of seasonal climate parameters in ice-core records, with emphasis on central Greenland, Journal of Glaciology, 44, 273–284, 1998.

Dansgaard, W.: Stable isotopes in precipitation, Tellus, 16, 436–468, https://doi.org/10.3402/tellusa.v16i4.8993, 1964.

Dansgaard, W., Johnsen, S., Clausen, H., and Gundestrup, N.: Stable isotope glaciology, Meddelelser om Gronland, 197, 1–53, 1973.

DeMonocal, P., Ortiz, J., Guilderson, T., and Sarnthein, M.: Coherent High- and Low-Latitude Climate Variability During the Holocene Warm Period, Science, 288, 2198–2202, 2000.

Fahlman, G. G. and Ulrych, T. J.: A new method for estimating the power spectrum of gapped data, Mon. Not. R. astr. Soc, 199, 53–65, 1982.

Fettweis, X., Box, J. E., Agosta, C., Amory, C., Kittel, C., Lang, C., van As, D., Machguth, H., and Gallée, H.: Reconstructions of the 1900-2015 Greenland ice sheet surface mass balance using the regional climate MAR model, The Cryosphere, 11, 1015–1033, https://doi.org/10.5194/tc-11-1015-2017, 2017.

https://doi.org/10.5194/cp-2020-19
Preprint. Discussion started: 24 February 2020

Fisher, D., Dyke, A., Koerner, R., Bourgeois, J., Kinnard, C., Zdanowicz, C., de Vernal, A., Hillaire-Marcel, C., Savelle, J., and Rochon, A.: Natural variability of Arctic sea ice over the Holocene, Eos, 87, 273–275, https://doi.org/10.1029/2006EO280001, 2006.

Frankcombe, L. M., von der Heydt, A., and Dijkstra, H. A.: North Atlantic Multidecadal Climate Variability: An Investigation of Dominant Time Scales and Processes, Journal of Climate, 23, 3626–3638, https://doi.org/10.1175/2010JCLI3471.1, 2010.

Gkinis, V., Popp, T. J., Blunier, T., Bigler, M., Schüpbach, S., Kettner, E., and Johnsen, S. J.: Water isotopic ratios from a continuously melted ice core sample, Atmospheric Measurement Techniques, 4, 2531–2542, https://doi.org/10.5194/amt-4-2531-2011, 2011.

Gkinis, V., Simonsen, S. B., Buchardt, S. L., White, J. W. C., and Vinther, B. M.: Water isotope diffusion rates from the NorthGRIP ice core for the last 16,000 years - Glaciological and paleoclimatic implications, Earth and Planetary Science Letters, 405, 132–141, https://doi.org/10.1016/j.epsl.2014.08.022, http://dx.doi.org/10.1016/j.epsl.2014.08.022, 2014.

Holme, C., Gkinis, V., Lanzky, M., Morris, V., Olesen, M., Thayer, A., Vaughn, B. H., and Vinther, B. M.: Varying regional δ^{18}O-temperature relationship in high-resolution stable water isotopes from east Greenland, Climate of the Past, 15, 893–912, 2019.

Hurrell, J. W. and Deser, C.: North Atlantic climate variability: The role of the North Atlantic Oscillation, Journal of Marine Systems, 78, 28–41, https://doi.org/10.1016/j.jmarsys.2008.11.026, http://dx.doi.org/10.1016/j.jmarsys.2008.11.026, 2009.

Huybers, P.: Combined obliquity and precession pacing of late Pleistocene deglaciations, Nature, 480, 229–232, https://doi.org/10.1038/nature10626, http://dx.doi.org/10.1038/nature10626, 2011.

Hwang, Y.-T. and Frierson, D. M.: Increasing atmospheric poleward energy transport with global warming, Geophysical Research Letters, 37, 1–5, https://doi.org/10.1029/2010GL045440, 2010.

Itagaki, K.: Self-Diffusion in Single Crystal Ice, Journal of the Physical Society of Japan, 22, 427–431, 1967.

Jakobsson, M., Long, A., Ingólfsson, Ó., Kjær, K. H., and Spielhagen, R. F.: New insights on Arctic Quaternary climate variability from palaeo-records and numerical modelling, Quaternary Science Reviews, 29, 3349–3358, https://doi.org/10.1016/j.quascirev.2010.08.016, http://dx.doi.org/10.1016/j.quascirev.2010.08.016, 2010.

Jean-Baptiste, P., Jouzel, J., Stievenard, M., and Ciais, P.: Experimental determination of the diffusion rate of deuterated water vapor in ice and application to the stable isotopes smoothing of ice cores, Earth and Planetary Science Letters, 158, 81–90, https://doi.org/10.1016/S0012-821X(98)00045-4, 1998.

Johnsen, S., Clausen, H., Dansgaard, W., Fuhrer, K., Gundestrup, N., Hammer, C., Iversen, P., Jouzel, J., Stauffer, B., and Steffensen, J.: Irregular glacial interstadials recorded in a new Greenland ice core, Nature, 359, 311–313, https://doi.org/10.1038/359311a0, 1992.

Johnsen, S., Clausen, H. B., Dansgaard, W., Gundestrup, N. S., Hammer, C. U., Andersen, U., Andersen, K. K., Hvidberg, C. S., Dahl-Jensen, D., Steffensen, J. P., Shoji, H., Sveinbjornsdottir, A. E., White, J., Jouzel, J., and Fisher, D.: The δ^{18}O record along the Greenland Ice Core Project deep ice core and the problem of possible Eemian climatic instability, Journal of Geophysical Research, 102, 26,397 – 26,410, 1997.

Johnsen, S. J., Clausen, H. B., Cuffey, K. M., Hoffmann, G., Schwander, J., and Creyts, T.: Diffusion of stable isotopes in polar firn and ice: the isotope effect in firn diffusion, Physics of Ice Core Records, pp. 121–140, 2000.

Jones, T., Cuffey, K., White, J., Steig, E., Buizert, C., Markle, B., McConnell, J., and Sigl, M.: Water isotope diffusion in the WAIS Divide ice core during the Holocene and last glacial, Journal of Geophysical Research: Earth Surface, pp. 290–309, https://doi.org/10.1002/2016JF003938, 2017a.

Jones, T. R., White, J. W. C., Steig, E. J., Vaughn, B. H., Morris, V., Gkinis, V., Markle, B. R., and Schoenemann, S. W.: Improved methodologies for continuous-flow analysis of stable water isotopes in ice cores, Atmospheric Measurement Techniques, 10, 617–632, https://doi.org/10.5194/amt-10-617-2017, 2017b.

https://doi.org/10.5194/cp-2020-19
Preprint. Discussion started: 24 February 2020

Jones, T. R., Roberts, W. H., Steig, E. J., Cuffey, K. M., Markle, B. R., and White, J. W.: Southern Hemisphere climate variability forced by Northern Hemisphere ice-sheet topography, Nature, 554, 351–355, https://doi.org/10.1038/nature24669, http://dx.doi.org/10.1038/nature24669, 2018.

Jouzel, J. and Merlivat, L.: Deuterium and Oxygen 18 in Precipitation: Modeling of the Isotopic Effects During Snow Formation, Journal of Geophysical Research, 89, 11 749–11 757, 1984.

Jouzel, J., Alley, R. B., Cuffey, K. M., Dansgaard, W., Grootes, G., Hoffmann, P., Johnsen, S. J., Koster, R. D., Peel, D., Shuman, C. A., Stievenard, M., Stuiver, M., and White, J.: Validity of the temperature reconstruction from water isotopes in ice cores, Journal of Geophysical Research, 102, 26 471–26 487, 1997.

Kahle, E. C., Holme, C., Jones, T. R., Gkinis, V., and Steig, E. J.: A Generalized Approach to Estimating Diffusion Length of Stable Water Isotopes From Ice-Core Data, Journal of Geophysical Research: Earth Surface, 123, 1–15, https://doi.org/10.1029/2018JF004764, 2018.

Knight, J. R., Allan, R. J., Folland, C. K., Vellinga, M., and Mann, M. E.: A signature of persistent natural thermohaline circulation cycles in observed climate, Geophysical Research Letters, 32, 1–4, https://doi.org/10.1029/2005GL024233, 2005.

Kuipers Munneke, P., Ligtenberg, S. R. M., Noël, B. P. Y., Howat, I. M., Box, J. E., Mosley-Thompson, E., McConnell, J. R., Steffen, K., Harper, J. T., Das, S. B., and Van Den Broeke, M. R.: Elevation change of the Greenland Ice Sheet due to surface mass balance and firn processes, 1960-2014, The Cryosphere, 9, 2009–2025, https://doi.org/10.5194/tc-9-2009-2015, 2015.

Merlivat, L. and Jouzel, J.: Global Climatic Interpretation of the Deuterium-Oxygen 18 Relationship for Precipitation, Journal of Geophysical Research, 84, 5029–5033, 1979.

Miller, G. H., Brigham-Grette, J., Alley, R. B., Anderson, L., Bauch, H. A., Douglas, M. S. V., Edwards, M. E., Elias, S. A., Finney, B. P., Fitzpatrick, J. J., Funder, S. V., Herbert, T. D., Hinzman, L. D., Kaufman, D. S., Macdonald, G. M., Polyak, L., Robock, A., Serreze, M. C., Smol, J. P., Spielhagen, R., White, J. W. C., Wolfe, A. P., and Wolff, E. W.: Temperature and precipitation history of the Arctic, Quaternary Science Reviews, 29, 1679–1715, https://doi.org/10.1016/j.quascirev.2010.03.001, http://dx.doi.org/10.1016/j.quascirev.2010.03.001, 2010.

Muilwijk, M., Smedsrud, L. H., Ilicak, M., and Drange, H.: Atlantic Water Heat Transport Variability in the 20th Century Arctic Ocean From a Global Ocean Model and Observations, Journal of Geophysical Research: Oceans, 123, 8159–8179, https://doi.org/10.1029/2018JC014327, 2018.

Müller, J., Werner, K., Stein, R., Fahl, K., Moros, M., and Jansen, E.: Holocene cooling culminates in sea ice oscillations in Fram Strait, Quaternary Science Reviews, 47, 1–14, https://doi.org/10.1016/j.quascirev.2012.04.024, 2012.

Noone, D. and Simmonds, I.: Sea ice control of water isotope transport to Antarctica and implications for ice core interpretation, Journal of Geophysical Research, 109, 1–13, https://doi.org/10.1029/2003JD004228, 2004.

Pawlowicz, R.: www.eoas.ubc.ca/~rich/map.html, 2020.

Polyak, L., Alley, R. B., Andrews, J. T., Brigham-Grette, J., Cronin, T. M., Darby, D. A., Dyke, A. S., Fitzpatrick, J. J., Funder, S., Holland, M., Jennings, A. E., Miller, G. H., Regan, M. O., Savelle, J., Serreze, M., St. John, K., White, J. W., and Wolff, E.: History of sea ice in the Arctic, Quaternary Science Reviews, 29, 1757–1778, https://doi.org/10.1016/j.quascirev.2010.02.010, http://dx.doi.org/10.1016/j.quascirev.2010.02.010, 2010.

Polyakov, I. V., Alekseev, G. V., Timokhov, L. A., Bhatt, U. S., Colony, R. L., Simmons, H. L., Walsh, D., Walsh, J. E., and Zakharov, V. F.: Variability of the Intermediate Atlantic Water of the Arctic Ocean over the Last 100 years, Journal of Climate, 17, 4485–4497, https://doi.org/10.1175/JCLI-3224.1, 2004.

Robin, G.: The Climatic Record from Ice Cores, in: The Climatic Record in Polar Ice Sheets, pp. 180–195, 1983.

https://doi.org/10.5194/cp-2020-19
Preprint. Discussion started: 24 February 2020

Saiz-Lopez, A., Blaszczak-Boxe, C. S., and Carpenter, L. J.: A mechanism for biologically induced iodine emissions from sea ice, Atmospheric Chemistry and Physics, 15, 9731–9746, https://doi.org/10.5194/acp-15-9731-2015, 2015.

Screen, J. A. and Simmonds, I.: The central role of diminishing sea ice in recent Arctic temperature amplification, Nature, 464, 1334–1337, https://doi.org/10.1038/nature09051, http://dx.doi.org/10.1038/nature09051, 2010.

Shindell, D. T., Schmidt, G. A., Mann, M. E., Rind, D., and Waple, A.: Solar Forcing of Regional Climate Change During the Maunder Minimum, Science, 294, 2149–2152, 2001.

Simonsen, M. F., Baccolo, G., Blunier, T., Borunda, A., Delmonte, B., Frei, R., Goldstein, S., Grinsted, A., Kjær, H. A., Sowers, T., Svensson, A., Vinther, B., Vladimirova, D., Winckler, G., Winstrup, M., and Vallelonga, P.: East Greenland ice core dust record reveals timing of Greenland ice sheet advance and retreat, Nature Communications, 10, https://doi.org/10.1038/s41467-019-12546-2, http://dx.doi.org/10.1038/s41467-019-12546-2, 2019.

Stevens, C. M., Verjans, V., Lundin, J. M. D., Kahle, E. C., Horlings, A. N., Horlings, B. I., and Waddington, E. D.: The Community Firn Model (CFM) v1.0, Geoscientific Model Development Discussions, 2020, 1–37, https://doi.org/10.5194/gmd-2019-361, https://www.geosci-model-dev-discuss.net/gmd-2019-361/, 2020.

Taranczewski, T., Freitag, J., Eisen, O., Vinther, B., Wahl, S., and Kipfstuhl, S.: 10,000 years of melt history of the 2015 Renland ice core, East Greenland, The Cryosphere Discussions, https://doi.org/10.5194/tc-2018-280, 2019.

Vinther, B., Buchardt, S., Clausen, H., Dahl-Jensen, D., Johnsen, S., Fisher, D., Koerner, R., Raynaud, D., Lipenkov, V., Andersen, K., Blunier, T., Rasmussen, S., Steffensen, J., and Svensson, A.: Holocene thinning of the Greenland ice sheet, Nature, 461, 385–388, https://doi.org/10.1038/nature08355, http://dx.doi.org/10.1038/nature08355, 2009.

Vinther, B. M., Johnsen, S. J., Andersen, K. K., Clausen, H. B., and Hansen, A. W.: NAO signal recorded in the stable isotopes of Greenland ice cores, Geophysical Research Letters, 30, 1–4, https://doi.org/10.1029/2002GL016193, 2003.

Vinther, B. M., Jones, P. D., Briffa, K. R., Clausen, H. B., Andersen, K. K., Dahl-Jensen, D., and Johnsen, S. J.: Climatic signals in multiple highly resolved stable isotope records from Greenland, Quaternary Science Reviews, 29, 522–538, https://doi.org/10.1016/j.quascirev.2009.11.002, http://dx.doi.org/10.1016/j.quascirev.2009.11.002, 2010.

Wanner, H., Mercolli, L., Grosjean, M., and Ritz, S. P.: Holocene climate variability and change; a data-based review, Journal of the Geological Society, 172, 254–263, https://doi.org/10.1144/jgs2013-101, 2015.

Whillans, I. and Grootes, P.: Isotopic diffusion in cold snow and firn, Journal of Geophysical Research, 90, 3910–3918, https://doi.org/10.1029/JD090iD02p03910, 1985.

Winstrup, M.: A Hidden Markov Model Approach to Infer Timescales for High-Resolution Climate Archives, in: Proceedings of the Thirtieth AAAI Conference on Artificial Intelligence, AAAI'16, pp. 4053–4060, AAAI Press, https://doi.org/10.5555/3016387.3016478, 2016.

Winstrup, M., Svensson, A. M., Rasmussen, S. O., Winther, O., Steig, E. J., and Axelrod, A. E.: An automated approach for annual layer counting in ice cores, Climate of the Past, 8, 1881–1895, https://doi.org/10.5194/cp-8-1881-2012, 2012.